

Single-Shot, Turbo Spin-Echo, Diffusion-Weighted Imaging versus Spin-Echo-Planar, Diffusion-Weighted Imaging in the Detection of Acquired Middle Ear Cholesteatoma

TECHNICAL NOTE

B. De Foer
J.-P. Vercruyse
B. Pilet
J. Michiels
R. Verriest
M. Pouillon
T. Somers
J.W. Casselman
E. Offeciers

SUMMARY: Diagnosis of acquired middle ear cholesteatoma on MR imaging is mostly done on late postgadolinium T1-weighted MR images and/or echo-planar (EPI) diffusion-weighted (DWI) MR images. We describe the appearance of a case of a complicated attic middle ear cholesteatoma on single-shot (SS) turbo spin-echo (TSE) DWI compared with EPI-DWI. This case suggests a higher reliability of SS TSE-DWI in the diagnosis of acquired middle ear cholesteatoma.

Diagnosis and extension of an acquired middle ear cholesteatoma is mainly done on thin-section, high-resolution CT. In selected cases, MR imaging has an additional value in describing possible complications of a middle ear cholesteatoma, such as extension to the lateral semicircular canal and other portions of the membranous labyrinth and the middle fossa through the eroded tegmen.¹ Recent reports have suggested the improvement in MR imaging techniques in diagnosing cholesteatoma with the use of delayed contrast-enhanced, T1-weighted MR images²⁻³ and echo-planar (EPI) diffusion-weighted (DWI) MR images^{1,4-8}. However, numerous artifacts can be generated during acquisition of DWI, such as eddy current artifacts, susceptibility artifacts, ghosting artifacts, chemical shift, and motion artifacts. With the use of higher magnetic fields, these artifacts and image distortions on EPI-DWI are even more pronounced.⁹⁻¹¹ Turbo spin-echo (TSE) DWI MR is known to lack significant image distortions and other artifacts. It permits fast multiplanar imaging in artifact-prone regions, such as the posterior fossa and the inferior frontal and temporal lobes.¹²

Case Report

A 76-year-old man presented with chronic ear discharge at the otorhinolaryngology department. Otoscopic findings revealed a tympanic membrane perforation and retraction with suspicion of a partially evacuated cholesteatoma. CT of the left ear revealed a soft tissue lesion (0.8 cm) in the attic with loss of the bony delineation of the anterior limb of the lateral semicircular canal (Fig 1) and the tegmen (Fig 2). Erosion of the incus body as well as the short and long process of the incus was noted (Fig 1). MR imaging was performed for evaluation of possible invasion into the membranous labyrinth and the middle cranial fossa. MR imaging was done on a 1.5T superconduc-

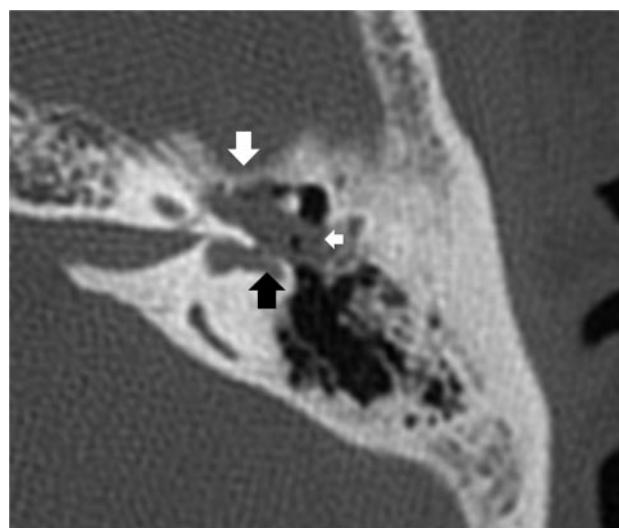


Fig 1. Axial high-resolution CT at the level of the lateral semicircular canal shows a nodular attic soft tissue lesion (*white arrow*) with erosion of the anterior limb of the lateral semicircular canal (*black arrow*), highly suggestive of a cholesteatoma with erosion of the anterior limb of the lateral semicircular canal. Note the loss of delineation of the body and short process of the incus suggesting an extensive erosion (*small arrow*).

tive system (Avanto; Siemens Medical Solutions, Erlangen, Germany). Imaging parameters are detailed in Table 1. Coronal thin-section, T2-weighted MR imaging revealed a slightly hyperintense nodular lesion under the tegmen delineated on its lateral side by clearly more hyperintense material (Fig 3). Late (45') postgadolinium T1-weighted MR imaging in the coronal plane showed a small, non-enhancing lesion surrounded by enhancing material mainly on its lateral side that was strongly suspected to be an attic, nonenhancing cholesteatoma (5 mm) surrounded by enhancing inflammatory tissue (Fig 4). No enhancement was noted in the membranous labyrinth or in the middle cranial fossa. On (B1000) EPI-DWI images, a curvilinear hyperintensity under the temporal lobe was seen on both sides. A clear nodular hyperintensity suspicious for a cholesteatoma could not be noted (Fig 5). The single-shot TSE-DWI showed no curvilinear hyperintensity at the air-bone interface of the temporal bone and obviously demonstrated a small nodular hyperintensity immediately

Received December 20, 2005; accepted after revision March 1, 2006.

From the Departments of Radiology (B.D.F., B.P., M.P., J.C.) and Otorhinolaryngology (R.V.) and University Department of Otorhinolaryngology (J.P.V., T.S., E.O.), A.Z. Sint-Augustinus, Antwerp, Belgium; Siemens Medical Solutions (J.M.), Anderlecht, Belgium; and the Department of Radiology (J.C.), A.Z. Sint-Jan AV, Bruges, Belgium.

Address correspondence to Bert De Foer, MD, Sint-Augustinus Hospital, Oosterveldlaan 24, 2610 Wilrijk, Belgium; e-mail: bert.defoer@GVAgroup.be

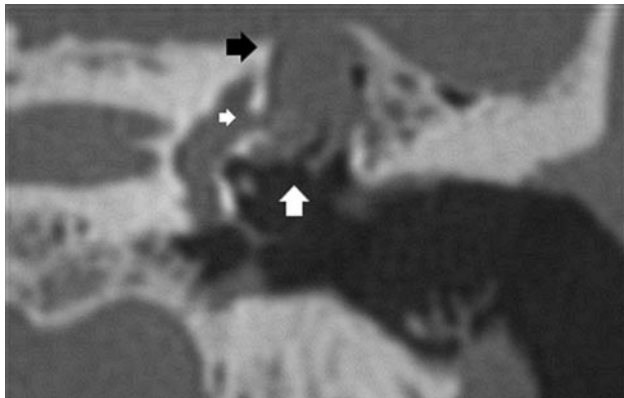


Fig 2. Coronal reformation of an axial volume spiral CT shows the attical soft-tissue lesion (*white arrow*) with loss of delineation of the tegmen (*black arrow*). Invasion into the middle cranial fossa cannot be excluded based on these images. There is also suspicion of a fistulization to the lateral semicircular canal on this coronal reformation (*small arrow*).

under the temporal lobe highly suggestive of a small cholesteatoma (Fig 6). On the basis of the late postgadolinium T1-weighted images and single-shot TSE-DWI, an attical cholesteatoma with surrounding inflammation without middle cranial fossa and membranous labyrinth invasion was diagnosed. Surgery confirmed the presence of a 5-mm large attical cholesteatoma surrounded by inflammation with erosion of the lateral semicircular canal but without invasion of the membranous labyrinth. The tegmen was thinned but not disrupted.

Discussion

Thin-section, high-resolution CT remains the primary imaging technique for the diagnosis and description of extension of a suspected middle ear cholesteatoma.¹ In selected cases, MR imaging has an additional value for the evaluation of cholesteatoma extension and for the assessment of possible complications such as erosion of the lateral semicircular canal, invasion of the membranous labyrinth, and invasion of the middle cranial fossa through an eroded tegmen.¹ Other complications, such as intracranial extension with temporal lobe abscess formation and facial nerve involvement can also be evaluated on MR imaging.¹ MR imaging is extremely useful for the demonstration and delineation of a temporal lobe en-

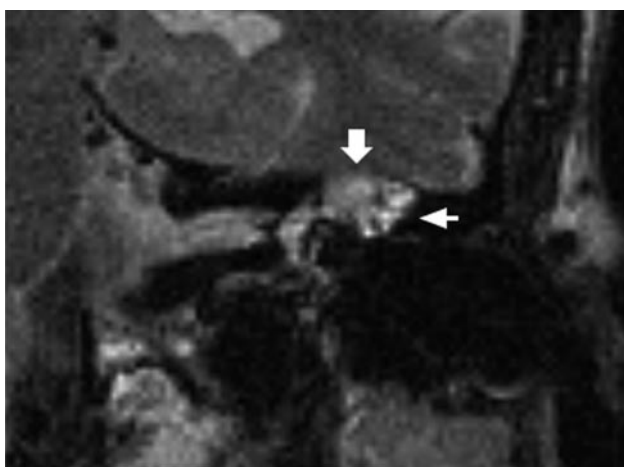


Fig 3. Coronal thin section T2-weighted MR image centered on the left ear reveals a nodular slightly hyperintense lesion (*large arrow*) under the temporal lobe with hyperintense material (*small arrow*) laterally, suggesting the presence of a small cholesteatoma with surrounding inflammatory tissue.

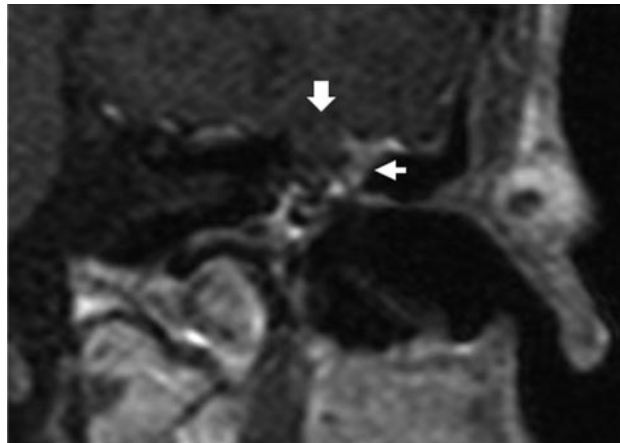


Fig 4. Coronal late postgadolinium T1-weighted MR image shows the cholesteatoma as a nonenhancing nodular lesion (*large arrow*) under the temporal lobe surrounded by enhancing inflammatory tissue (*small arrow*) mainly on its lateral side.

cephalocele in the case of a deficient tegmen.¹ MR imaging is able to discriminate the nonenhancing cholesteatoma from enhancing inflammatory or granulation tissue.¹³ Several reports have discussed the appearance of acquired cholesteatoma on late postgadolinium T1-weighted MR images^{2,3} and on EPI-DWI images.^{1,4-8} On EPI-DWI, cholesteatomas demonstrate a hyperintensity probably based on a T2 shine-through effect.^{4,8} However, a major limitation of the EPI-DWI images still seems to be the important susceptibility artifact at the skull base (among other artifacts), the low resolution, and relatively thick sections,⁹⁻¹¹ thus causing a size limit for detection on EPI-DWI of approximately 5 mm.^{5,7,8} Susceptibility artifacts caused by field inhomogeneities at the air-bone interface of the temporal bone can be reduced with the use of parallel imaging techniques.^{11,14} Other acquisition sequences that are less sensitive to susceptibility artifacts, such as multishot EPI sequences, spin-echo EPI sequences, and flash sequences, can be used.¹¹

Single-shot TSE-DWI uses a 180° radio-frequency refocusing pulse for each measured echo, which explains the reduction of the susceptibility artifact. It allows the use of a higher imaging matrix and thinner sections (2 mm). Our case sug-

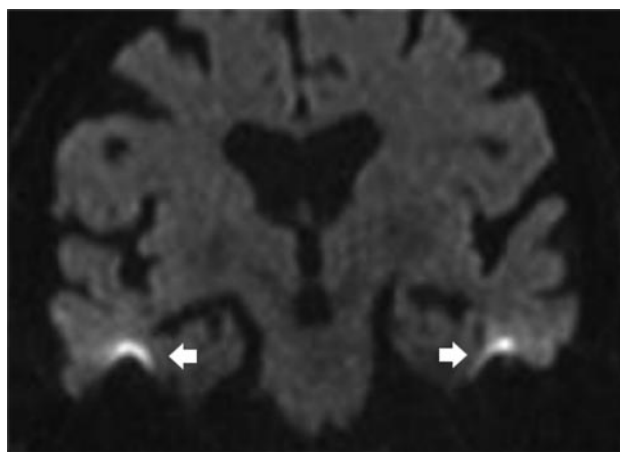


Fig 5. Coronal EPI-DWI shows a bilateral curvilinear hyperintensity (*white arrows*) under the temporal lobe, compatible with a large susceptibility artifact. No nodular hyperintensity suggestive of cholesteatoma can be seen.

Detailed description of imaging parameters

Sequence Name	Orientation	TR (ms)	TE (ms)	Section (mm)	Matrix	FOV (mm)
EPI DWI	Coronal	3000	82	3	128 × 128	128 × 170
SS TSE DWI	Coronal	2000	115	2	134 × 192	220 × 220
TSE T1WI	Coronal/transverse	450	17	2	192 × 256	128 × 170
TSE T2-WI	Coronal	3500	92	2	192 × 256	128 × 170

Note:—EPI indicates echo-planar imaging; DWI, diffusion-weighted MR imaging; SS, single-shot; TSE, turbo spin-echo; T1WI, T1-weighted imaging; T2WI, T2-weighted imaging, TR, repetition time; TE, echo time; FOV, field of view.

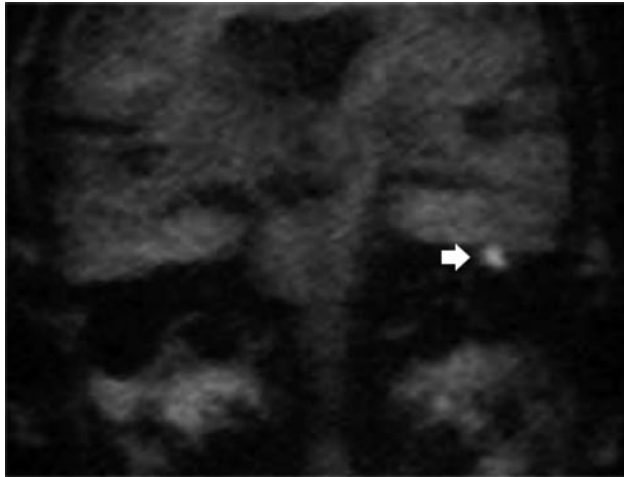


Fig 6. Coronal single-shot TSE-DWI shows no curvilinear interface artifact but clearly demonstrates a hyperintensity under the temporal lobe, indicating that a cholesteatoma is present (white arrow).

gests that single-shot TSE-DWI with an actual size of 2 mm is able to discriminate smaller cholesteatomas. In this particular case, because of the absence of susceptibility artifacts at the interface between temporal lobe and temporal bone, the cholesteatoma could obviously be depicted. This demonstrates the advantage of this sequence. The size of the actual cholesteatoma at surgery was 5 mm. It was surrounded by inflammatory tissue. Furthermore, the late postgadolinium T1-weighted images also succeeded in differentiating the nonenhancing cholesteatoma from the surrounding enhancing inflammatory and granulation tissue.

Although in this case the combination of late postgadolinium T1-weighted images and single-shot TSE-DWI proved to be very convincing for the diagnosis of a primary acquired cholesteatoma, further studies on larger series are needed to

prove the value of single-shot TSE-DWI in combination with late postgadolinium T1-weighted images for the diagnosis of primary acquired and residual cholesteatoma.

References

1. Lemmerling M, De Foer B. **Imaging of cholesteatomatous and non-cholesteatomatous middle ear disease.** In: Lemmerling M, Kollias SS, eds. *Radiology of the Petrous Bone*. New York: Springer-Verlag; 2004:31–47
2. Williams MT, Ayache D, Alberti C, et al. **Detection of postoperative residual cholesteatoma with delayed-contrast-enhanced MR imaging: initial findings.** *Eur Radiol* 2003;13:169–74
3. Ayache D, Williams MT, Lejeune D, et al. **Usefulness of delayed postcontrast magnetic resonance imaging in the detection of residual cholesteatoma after canal wall-up tympanoplasty.** *Laryngoscope* 2005;115:607–10
4. Fitzek C, Mewes T, Fitzek S, et al. **Diffusion-weighted MRI of cholesteatomas of the petrous bone.** *J Magn Reson Imaging* 2002;15:636–41
5. Aikele P, Kittner T, Offergeld C, et al. **Diffusion-weighted MR imaging of cholesteatoma in pediatric and adult patients who have undergone middle ear surgery.** *Am J Roentgenol* 2003;181:261–65
6. Maheshwari S, Mukherji SK. **Diffusion-weighted imaging for differentiating recurrent cholesteatoma from granulation tissue after mastoidectomy: case report.** *AJNR Am J Neuroradiol* 2002;23:847–49
7. Stassola A, Magliulo G, Parrotto D, et al. **Detection of postoperative relapsing/residual cholesteatoma with diffusion-weighted echo-planar magnetic resonance imaging.** *Otol Neurotol* 2004;25:879–84
8. Vercruyse JP, De Foer B, Pouillon M, et al. **The value of diffusion-weighted MR-imaging in the diagnosis of primary acquired and residual cholesteatoma: a surgical verified study in 100 patients.** *Eur Radiol* Mar 3, 2006 (Epub).
9. Fisher H, Ladebeck R. **Echo planar imaging image artifacts.** In: Schmitt F, Stehling MK, Turner R, eds. *Echo-Planar Imaging: Theory, Technique and Application*. New York: Springer-Verlag; 1998:179–200
10. Bammer R. **Basic principles of diffusion-weighted imaging.** *Eur Radiol* 2003; 45:169–84
11. Hiwatashi A, Zhong J. **Pitfalls and artifacts of DW imaging.** In: Moritani T, Ekholm S, Westesson PL, eds. *Diffusion-Weighted MR Imaging of the Brain*. New York: Springer-Verlag; 2005:11–24
12. Lövblad KO, Jakob PM, Qun C, et al. **Turbo spin-echo diffusion-weighted MR of ischemic stroke.** *AJNR Am J Neuroradiol* 1998;19:201–08
13. Martin N, Sterkers O, Nahum M. **Chronic inflammatory disease of the middle ear cavities: Gd-DTPA-enhanced MR imaging.** *Radiology* 1990;176:399–405
14. Van Den Brink JS, Watanabe Y, Kuhl CK, et al. **Implications of SENSE MR in routine clinical practice.** *Eur J Radiol* 2003;46:3–27